Biochemical and Biophysical Research Communications 463 (2015) 389–394

Contents lists available at ScienceDirect

Biochemical and Biophysical Research Communications

journal homepage: www.elsevier.com/locate/ybbrc

Ablation of Dicer leads to widespread perturbation of signaling pathways

Nandini A. Sahasrabuddhe [a, b], Tai-Chung Huang [c], Praveen Kumar [a], Yi Yang [c], Bidyut Ghosh [g], Steven D. Leach [c, g, h], Raghothama Chaerkady [a, b, c], Akhilesh Pandey [a, c, d, e, f, *]

[a] Institute of Bioinformatics, International Technology Park, Bangalore 560066, India
[b] Manipal University, Madhav Nagar, Manipal 576104, India
[c] McKusick-Nathans Institute of Genetic Medicine, Johns Hopkins University School of Medicine, Baltimore, MD 21205, USA
[d] Department of Biological Chemistry, Johns Hopkins University School of Medicine, Baltimore, MD 21205, USA
[e] Department of Pathology, Johns Hopkins University School of Medicine, Baltimore, MD 21205, USA
[f] Department of Oncology, Johns Hopkins University School of Medicine, Baltimore, MD 21205, USA
[g] Department of Surgery, Johns Hopkins University School of Medicine, Baltimore, MD 21205, USA
[h] Rubenstein Center for Pancreatic Cancer Research, Memorial Sloan-Kettering Cancer Center, New York, NY 10065, USA

ARTICLE INFO

Article history:
Received 23 April 2015
Accepted 15 May 2015
Available online 30 May 2015

Keywords:
Dicer
Phosphotyrosine
Pathways
Receptor tyrosine kinase
SILAC

ABSTRACT

Dicer is an essential ribonuclease involved in the biogenesis of miRNAs. Previous studies have reported downregulation of Dicer in multiple cancers including hepatocellular carcinoma. To identify signaling pathways that are altered upon Dicer depletion, we carried out quantitative phosphotyrosine profiling of liver tissue from Dicer knockout mice. We employed antibody-based enrichment of phosphotyrosine containing peptides coupled with SILAC spike-in approach for quantitation. High resolution mass spectrometry-based analysis identified 349 phosphotyrosine peptides corresponding to 306 unique phosphosites of which 75 were hyperphosphorylated and 78 were hypophosphorylated. Several receptor tyrosine kinases including MET, PDGF receptor alpha, Insulin-like growth factor 1 and Insulin receptor as well as non-receptor tyrosine kinases such as Src family kinases were found to be hyperphosphorylated upon depletion of Dicer. In addition, signaling molecules such as IRS-2 and STAT3 were hyperphosphorylated. Activation of these signaling pathways has been implicated previously in various types of cancers. Interestingly, we observed hypophosphorylation of molecules including focal adhesion kinase and paxillin. Our study profiles the perturbed signaling pathways in response to dysregulated miRNAs resulting from depletion of Dicer. Our findings warrant further studies to investigate oncogenic effects of downregulation of Dicer in cancers.

1. Introduction

Dicer is a ribonuclease involved in the biogenesis of miRNAs and RNA silencing. It is required for growth and development and its deficiency causes embryonic lethality [1,2]. As miRNAs are key mediators of post-transcriptional gene regulation, lack of Dicer leads to dysregulation of Dicer-dependent miRNAs, which subsequently impacts the downstream transcriptome and proteome. It has been demonstrated that Dicer regulates various cellular processes including proliferation, differentiation and regulation of metabolism [3–5]. Interestingly, downregulation of Dicer is shown to associate with tumorigenesis and metastasis, and lower expression of Dicer is observed in various types of cancers such as lung, ovarian and liver cancers [6–8] Han et al. have demonstrated activation of Akt upon ablation of Dicer [9]. Hypoxia-mediated downregulation of Dicer was observed to lead expression of several hypoxia associated factors including HIF-α, a process known to be associated with cancer development [10]. Taken together, these studies suggest that there might be a more global dysregulation of signaling pathways upon ablation of Dicer.

One of the key protein post-translational modifications in signal transduction is the phosphorylation of tyrosine residues.

* Corresponding author. McKusick-Nathans Institute of Genetic Medicine, 733 N. Broadway, BRB 527, Johns Hopkins University, Baltimore, MD 21205, USA.
E-mail address: pandey@jhmi.edu (A. Pandey).

http://dx.doi.org/10.1016/j.bbrc.2015.05.077
0006-291X/

Phosphotyrosine signaling controls various cellular processes, cell–cell and cell–environment interactions. With an established association of downregulation of Dicer with various types of cancer, we sought to investigate the phosphotyrosine proteome downstream of Dicer. Owing to its low abundance, anti-phosphotyrosine antibody-based enrichment methods have been developed to increase the detection of tyrosine phosphoproteome [11]. To quantify the enriched phosphotyrosine-containing peptides, a variety of methods have been established. As *in vitro* labeling such as iTRAQ or label-free methods are more prone to introducing experimental errors, the SILAC approach for the metabolic labeling now is widely adopted [12]. Recently, SILAC spike-in approach was developed, where SILAC labeled cell lysates are spiked at a fixed ratio for relative quantitation [13]. In principle, the spiked-in peptides serve as the internal reference standards to compare the relative abundance of phosphopeptides.

To understand the *in vivo* alterations of the phosphotyrosine-mediated signaling associated with Dicer depletion, we employed SILAC spike-in approach. We carried out replicate analysis of unlabeled liver lysates of control and Dicer knockout mice spiked with SILAC labeled Hepa 1–6 cell lysates. High resolution mass spectrometry-based analysis identified 306 phosphotyrosine sites, of which 75 were hyperphosphorylated. We further carried out bioinformatics revealed enrichment of pathways such as MET and IGF1R which are associated with oncogenesis. Our findings shed light on possible association of downregulation of Dicer and activation of oncogenic signaling pathways.

2. Material and methods

2.1. Generation of Dicer knockout mice and SILAC labeled Hepa 1–6 cells

We selected Cre-loxP system to generate inducible knockout mice, as described previously [5]. In brief, ROSA26-CreERT2 mice and mice with floxed Dicer exons 21 and 22 were crossed. Administration of tamoxifen resulted in deletion of floxed *Dicer* exon 21 and 22. On the day 8 post-induction, mice were starved for 3 h prior to euthanasia and necropsy to harvest liver from 5 Dicer knockout mice. Similarly, 5 uninduced control mice were also starved prior to euthanasia and necropsy. Mouse hepatoma Hepa 1–6 cells were (kind gift from Kensler Lab, School of Public Health, Johns Hopkins University) adapted to $^{13}C_6$-Lysine; $^{13}C_6$-Arginine containing custom DMEM media to label proteins *in vivo*.

2.2. In-solution trypsin digestion

Lysates were prepared in urea lysis buffer containing 20 mM HEPES pH 8.0, 9 M urea, 1 mM sodium orthovanadate, 2.5 mM sodium pyrophosphate and 1 mM β-glycerophosphate supplemented with Complete protease inhibitor cocktail (Roche Diagnostic Systems). The lysates were sonicated and cleared by centrifugation at 3000 × g at 4 °C for 10 min. Protein estimation was carried out using BCA protein assay. Equal amount of protein was pooled from each mouse to obtain pooled control and pooled Dicer knockout liver lysates. ~30 mg protein from each pooled sample (spiked with SILAC labeled Hepa 1–6 lysate at 5:1 w:w ratio) was reduced with 5 mM dithiothreitol and alkylated with 10 mM iodoacetamide. *In-solution* digestion was carried out using TPCK-treated trypsin on an orbital shaker at 25 °C overnight. The protein digest was desalted using SepPak C18 cartridge (Waters Incorporation, USA) and eluted peptides were lyophilized for phosphotyrosine peptide enrichment.

2.3. Anti-phosphotyrosine Western blot and immunoaffinity enrichment of phosphotyrosine peptides

Phosphotyrosine protein profile of liver from control and Dicer knockout mice was analyzed by Western blot using 4G10 anti-phosphotyrosine antibody essentially as described before [14].

For immunoaffinity enrichment, the lyophilized peptides were reconstituted in 1.4 ml of immunoaffinity purification (IAP) buffer

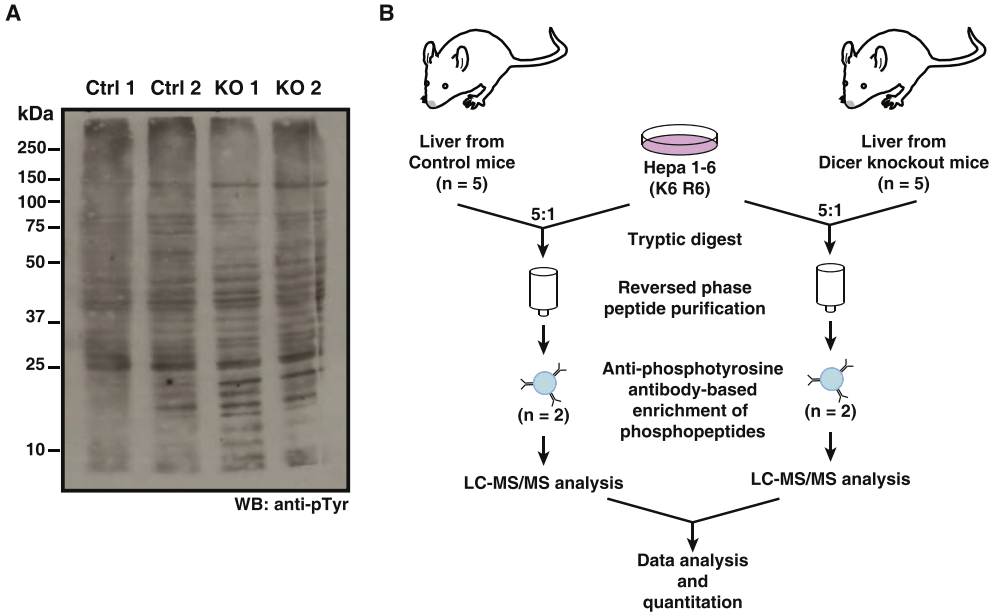

Fig. 1. Investigation of phosphotyrosine profile upon ablation of Dicer A) Phosphotyrosine profile of control and Dicer knockout mice. Ctrl1 and Ctrl2 represent liver lysates from two control mice and KO 1 and KO 2 represent liver lysates from 2 Dicer knockout mice. The lysates were immunoblotted using anti-phosphotyrosine antibody. B) Schematic representation of workflow followed to identify differentially phosphorylated tyrosine sites upon ablation of Dicer. Pooled liver lysates from 5 control and 5 Dicer knockout mice were spiked with $^{13}C_6$-lysine and $^{13}C_6$-ariginine labeled Hepa 1–6 cell lysates and replicate analysis was carried out. Phosphotyrosine containing peptides were enriched using pY100 anti-phosphotyrosine antibody. LC-MS/MS analysis was carried out using LTQ-Orbitrap Velos followed by data analysis.

containing 50 mM MOPS pH 7.2, 10 mM sodium phosphate, 50 mM NaCl. Anti-phosphotyrosine antibody pY100 (Cat # 5636S, Cell Signaling Technology, MA) and peptide solution was incubated on a rotator at 4 °C for 30 min followed by centrifugation at 1500 × g for 1 min. It was followed by two washes with IAP buffer and twice with water. Phosphopeptides were eluted using 0.1% TFA. The eluted phosphopeptide sample was desalted using C_{18} STAGE tips as carried out previously, vacuum dried and stored at −80 °C until LC-MS/MS analysis [15].

2.4. LC-MS/MS and data analysis

LC-MS/MS analysis of enriched phosphopeptides was carried out using Eksigent nanoflow liquid chromatography interfaced with an LTQ-Orbitrap Velos mass spectrometer (Thermo Scientific, San Jose, CA). The peptides were loaded onto a 2 cm × 75 μm, Magic C_{18} AQ 5 μm, 120 Å trap column at a flow rate of 3 μl/min using 0.1% formic acid for enrichment. The peptides were separated on an analytical column (10 cm × 75 μm, Magic C_{18} AQ 5 μm, 120 Å) by a linear gradient from 5 to 60% ACN in 90 min. MS and MS/MS scans were acquired at resolving power of 60,000 and 15.000 at 400 *m*/*z*, respectively. HCD fragmentation of the 10 most abundant ions was carried out in a data dependent manner (isolation width: 1.90 *m*/*z*; normalized collision energy: 35%). The tandem mass spectrometry data were searched using MASCOT (v 2.2) and SEQUEST search algorithms against a mouse RefSeq database (RefSeq 42) supplemented with frequently observed contaminants through the Proteome Discoverer platform (v1.2, Thermo Scientific, Bremen, Germany). For both algorithms, the search parameters included a maximum of two missed cleavage; carbamidomethylation at cysteine as a fixed modification; protein N-terminal acetylation, deamidation at asparagine and glutamine, oxidation at methionine, phosphorylation at serine, threonine and tyrosine and SILAC labels $^{13}C_6$-Lysine; $^{13}C_6$-Arginine as variable modifications. The MS error tolerance was set at 10 ppm and MS/MS error tolerance to 0.05 Da. The peptides with maximum of 2 missed cleavage that scored better than the score cut-off for 1% false discovery rate were considered for further analysis [16]. The peak area and quantitation ratio for each phosphopeptide-spectrum match was calculated by the quantitation node and the probability of phosphorylation for each S/T/Y site on each peptide was calculated by the PhosphoRS node (Version 3.0) in the Proteome Discoverer [17]. Peptides with ≥75% phosphosites probability were considered for further analysis. The data have been deposited to the ProteomeXchange Consortium via the PRIDE partner repository with the dataset identifier PXD000927.

To identify enriched protein–protein interaction networks and pathways amongst the hyperphosphorylated proteins (≥1.5 − fold), we carried out Ingenuity Pathway Analysis (IPA®, QIAGEN Redwood City, www.qiagen.com/ingenuity) and DAVID [18]. Using the hyperphosphorylated proteins as an input, NetworKIN algorithm was used to predict the upstream kinases [19].

3. Results and discussion

3.1. Perturbation of tyrosine phosphoproteome upon ablation of Dicer

To investigate Dicer mediated alterations of tyrosine phosphoproteome, we initially assessed the phosphotyrosine profile of liver

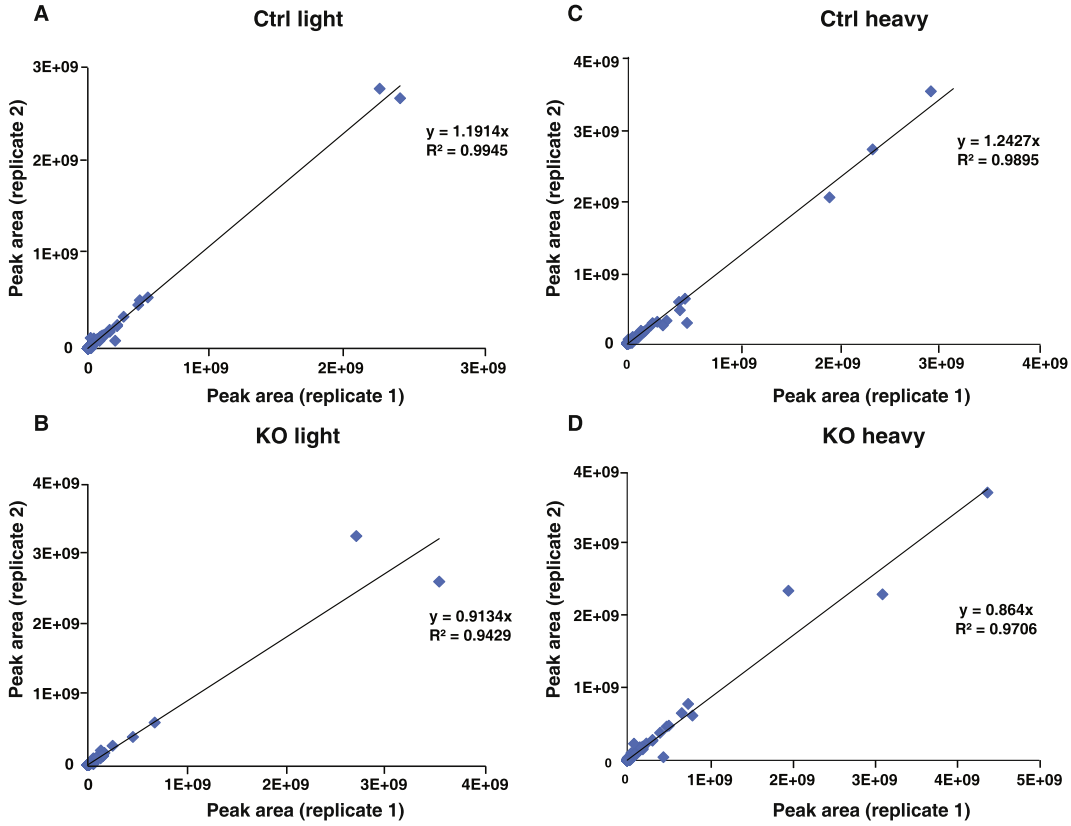

Fig. 2. Correlation plot of the peak areas of phosphopeptides A–B) Correlation plot of peak areas of heavy phosphopeptides identified in replicate analysis of control mice (Ctrl) (panel A) and Dicer knockout mice (KO) (panel B). C–D) Correlation plot of peak areas of light phosphopeptides identified in common between replicate analysis of control mice (Ctrl) (panel C) and Dicer knockout mice (KO) (panel D).

lysates from control and Dicer knockout mice using anti-phosphotyrosine antibody-based immunoblotting. Upon ablation of Dicer, alteration in the phosphotyrosine profile was observed as shown in Fig. 1A. To understand the modulated signaling in Dicer knockout mice, we carried out replicate analysis of unlabeled liver lysates of control and Dicer knockout mice spiked with SILAC labeled Hepa 1–6 cell lysates as depicted in Fig. 1B. Enrichment of phosphotyrosine peptides was carried out using anti-phosphotyrosine antibody. High resolution mass spectrometry-based analysis was carried out using LTQ Orbitrap Velos.

To check if the spike-in heavy peptides served as suitable internal standards and assess the reproducibility of the analysis, we calculated the regression coefficient of phosphopeptide peak areas between replicates. As shown in Fig. 2A–D, peak areas of both light and heavy phosphopeptides in knockout and control mouse samples were reproducible and the correlation coefficients were all greater than 0.9. Overall, we identified 502 unique phosphotyrosine peptides in replicates of control and 447 in replicates of Dicer knockout mice. To identify the dysregulated phosphosites in Dicer knockout mice, we calculated the ratio of average peak areas of phosphopeptides between Dicer knockout and control mice. As listed in Supplementary Tables I and 349 phosphotyrosine peptides corresponding to 306 unique phosphosites were identified in common amongst control and Dicer knockout samples. Of the 306 phosphotyrosine sites, 75 were hyperphosphorylated ($\geq$1.5-fold) and 78 were hypophosphorylated ($\geq$1.5-fold) in Dicer knockout mouse liver.

3.2. Hyperphosphorylation of kinome and signaling molecules upon ablation of Dicer

The hyperphosphorylated 75 phosphosites corresponded to 61 proteins. These included receptor tyrosine kinases such as Eph receptor B3 (7.5-fold), PDGF receptor alpha (7.3-fold), Met (4-fold), Insulin-like growth factor 1 and Insulin receptors (1.7-fold). The non-receptor tyrosine kinases included Src family kinases like Fgr (7.3-fold). Table 1 shows a representative list of hyperphosphorylated phosphosites in Dicer knockout mice. Representative MS and MS/MS spectra of hyperphosphorylated phosphopeptide from tyrosine kinase Fgr are depicted in Fig. 3A. The enriched pathways amongst the hyperphosphorylated phosphoproteins included Met and IGF1R pathways. Y1233 of Met, which was hyperphosphorylated upon Dicer depletion, is important for autophosphorylation, dimerization and biological activity of Met [20]. Insulin-like growth factor 1 receptor (Igf1r) and Insulin receptor (Insr) can form heterodimers. Activation of Igf1r can activate Pi3k/Akt pathway stimulating cell growth and proliferation. Igf1r and Insr contain homologous tyrosine kinase domain, within which several tyrosine residues crucial for activation are conserved. Among them, we observed hyperphosphorylation of Y1167 (1.7-fold) which is an autophosphorylation site involved in regulation of Src. Representative MS and MS/MS spectra for the phosphopeptide are depicted in Supplementary Fig. 1A. Supplementary Fig. 1B illustrates the observed interaction network of Igf1r in Dicer knockout mice.

Downstream signaling partners of these receptor tyrosine kinases were also observed to be hyperphosphorylated. Mitogen-activated protein kinase 1 and 3 were hyperphosphorylated at Y185 [1.7-fold] and Y205 [1.7-fold], respectively. Signal transducer and activator of transcription 3 (Stat3) a key downstream effector of multiple receptor tyrosine kinases binds to Met and is activated upon phosphorylation at Y705 (5.7- fold hyperphosphorylated). Fig. 3B illustrates the interaction network of hyperphosphorylated signaling partners in Dicer knockout mice.

3.3. Depletion of Dicer leads to hypophosphorylation of focal adhesion pathway partners

Interestingly, amongst the hypophosphorylated proteins, focal adhesion pathway was the most enriched. We observed hypophosphorylation of molecules involved in adhesion and cell motility such as focal adhesion kinase (Ptk2) and paxillin (Pxn). Y925, Y577 and Y397 which are crucial for activation and downstream signaling of Ptk2 were hypophosphorylated upon Dicer ablation. Reduction of phosphorylation of Ptk2 upon down-regulation of Dicer has been reported previously by Asada et al. [21]. Tyrosine −118 of Pxn, substrate site of Ptk2 was also observed to be hypophosphorylated in Dicer knockout mice [22]. Breast cancer anti-estrogen resistance 1, a cas family docking protein, was hypophosphorylated at multiple sites in liver of Dicer knockout mice including Y271 and Y253 reported to be involved in cell motility and tumorigenesis. These observations indicate that Dicer ablation possibly perturbed activity of molecules involved in the focal adhesion pathway.

3.4. Upstream kinase analysis

We further carried out upstream kinases prediction using NetworKIN algorithm based on the known kinase substrate motifs in the literature [19]. Y1354 of Met was correctly predicted as an autophosphorylation site. Igf1r/Insr and Eph receptors were enriched as upstream kinases. Some of the predicted substrates for

Table 1
A representative list of hyperphosphorylated tyrosine sites in Dicer knockout mice. This table lists phosphotyrosine peptide, Ion score, Xcorr, phosphoRS probability, corresponding proteins, gene symbol, phosphosite and Dicer knockout/control fold change.

	Phosphopeptide	Ion score[b]	Xcorr[b]	phosphoRS probability[b]	Protein	Gene symbol	Phosphosite	Dicer KO/control
1	SYIGSNHSSLGSMSPSNMEG[Y]SK[a]	69	5.83	1.0	Coxsackie virus and adenovirus receptor	*Cxadr*	Y313	7.8
2	VYIDPFT[Y]EDPNEAVR	86	3.5	1.0	Eph receptor B3	*Ephb3*	Y605	7.5
3	KLDTGG[Y]YITTR	79	3.8	1.0	Gardner-Rasheed feline sarcoma viral (Fgr) oncogene homolog	*Fgr*	Y196	7.3
4	SL[Y]DRPAS[Y]K	54	3.35	1.0	Platelet derived growth factor receptor, alpha	*Pdgfra*	Y762, Y768	7.3
5	SAVTTVVNPK[Y]EGK	70	3.88	1.0	Integrin beta 1	*Itgb1*	Y795	5.8
6	YCRPESQEHPEADPGSAAP[Y]LK	–	3.13	1.0	Signal transducer and activator of transcription 3	*Stat3*	Y705	5.7
7	WPTVDASY[Y]GGR	56	3.16	1.0	Anthrax toxin receptor 2	*Antxr2*	Y381	5.5
8	DMYDKEY[Y]SVHNK	63	3.23	1.0	Met proto-oncogene	*Met*	Y1233	4.0
9	EVE[Y]SDKHGQYLIGHGTK	91	3.91	1.0	Eph receptor B4	*Ephb4*	Y583	3.3
10	SRPPYTD[Y]VSTR	57	3.43	1.0	Intestinal cell kinase	*Ick*	Y159	3.2

[a] [Y] denotes identified phosphotyrosine.
[b] Representative from one of the control replicates.

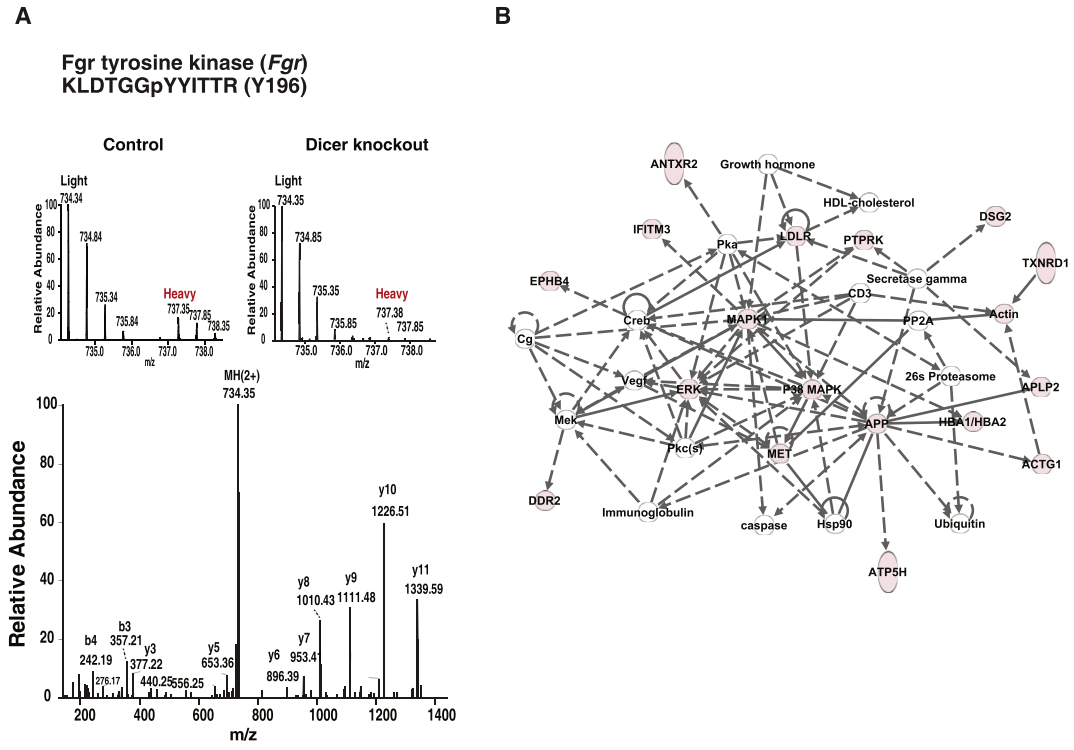

Fig. 3. Activation of several signaling pathways upon depletion of Dicer A) MS and MS/MS spectra of hyperphosphorylated tyrosine site from Fgr in Dicer knockout mice. Top panel shows MS showing hyperphosphorylation in Dicer knockout mice and the bottom panel shows MS/MS of KLDTGGpYYITTR. B) Enrichment of multiple signaling molecules involved in proliferation and tumorigenesis in liver of induced Dicer knockout mice Network diagram illustrates crosstalk of multiple receptor tyrosine kinases such as EPHA2, PDGFRα, MET and downstream signaling mediators activated in liver of induced Dicer knockout mice. Nodes colored in pink denote hyperphosphorylated proteins in Dicer knockout mice. (For interpretation of the references to color in this figure legend, the reader is referred to the web version of this article.)

Igf1r include Irs-2 (Y671), Fgr (Y196), Dsg2 (Y971) and Lyn (Y316). Both our data and the NetworKIN prediction point to the enrichment of Igf1r/Insr signaling pathway upon ablation of Dicer.

As reported earlier, liver-specific knockdown of Dicer in mice, resulted in tumor development over a year and Dicer was also observed to be downregulated in HCC [8,23]. The hyperphosphorylated receptor tyrosine kinases including Met, PDGF receptor alpha (Pdgfrα) and Igf1r/Insr identified in our study have been reported to be associated with HCC. Several drugs are in clinical trials targeting Met in HCC patients [24]. *IGF1R* is reported to be amplified in hepatocellular carcinoma [25].

In summary, our findings indicate that downregulation of Dicer possibly leads to activation of multiple pathways downstream of receptor tyrosine kinase signaling, but also leads to deactivation of pathways such as focal adhesion which is crucial for cell migration. Thus, it appears that other oncogenic changes act along with depletion of Dicer to shift the balance towards activation of oncogenic signaling pathways in cancers. Further studies are warranted to identify the dysregulated Dicer-dependent miRNAs and their contribution to aberrant signaling pathways.

Acknowledgments

This work was supported by NCI's Clinical Proteomic Tumor Analysis Consortium Initiative (U24CA160036), an NIH roadmap grant for Technology Centers of Networks and Pathways (U54GM103520) and a contract (HHSN268201000032C) from the National Heart, Lung and Blood Institute.

Appendix A. Supplementary data

Supplementary data related to this article can be found at http://dx.doi.org/10.1016/j.bbrc.2015.05.077.

Transparency document

Transparency document related to this article can be found online at http://dx.doi.org/10.1016/j.bbrc.2015.05.077.

References

[1] J.M. Calabrese, A.C. Seila, G.W. Yeo, P.A. Sharp, RNA sequence analysis defines Dicer's role in mouse embryonic stem cells, Proc. Natl. Acad. Sci. U. S. A. 104 (2007) 18097–18102.
[2] E. Bernstein, S.Y. Kim, M.A. Carmell, E.P. Murchison, H. Alcorn, M.Z. Li, A.A. Mills, S.J. Elledge, K.V. Anderson, G.J. Hannon, Dicer is essential for mouse development, Nat. Genet. 35 (2003) 215–217.
[3] L. Lei, S. Jin, G. Gonzalez, R.R. Behringer, T.K. Woodruff, The regulatory role of Dicer in folliculogenesis in mice, Mol. Cell. Endocrinol. 315 (2010) 63–73.
[4] H.M. Korhonen, O. Meikar, R.P. Yadav, M.D. Papaioannou, Y. Romero, M. Da Ros, P.L. Herrera, J. Toppari, S. Nef, N. Kotaja, Dicer is required for haploid male germ cell differentiation in mice, PLoS One 6 (2011) e24821.
[5] T.C. Huang, N.A. Sahasrabuddhe, M.S. Kim, D. Getnet, Y. Yang, J.M. Peterson, B. Ghosh, R. Chaerkady, S.D. Leach, L. Marchionni, G.W. Wong, A. Pandey, Regulation of lipid metabolism by dicer revealed through SILAC mice, J. Proteome Res. 11 (2012) 2193–2205.
[6] Y. Karube, H. Tanaka, H. Osada, S. Tomida, Y. Tatematsu, K. Yanagisawa, Y. Yatabe, J. Takamizawa, S. Miyoshi, T. Mitsudomi, T. Takahashi, Reduced expression of Dicer associated with poor prognosis in lung cancer patients, Cancer Sci. 96 (2005) 111–115.
[7] W.M. Merritt, Y.G. Lin, L.Y. Han, A.A. Kamat, W.A. Spannuth, R. Schmandt, D. Urbauer, L.A. Pennacchio, J.F. Cheng, A.M. Nick, M.T. Deavers, A. Mourad-Zeidan, H. Wang, P. Mueller, M.E. Lenburg, J.W. Gray, S. Mok, M.J. Birrer, G. Lopez-Berestein, R.L. Coleman, M. Bar-Eli, A.K. Sood, Dicer, Drosha, and

outcomes in patients with ovarian cancer, N. Engl. J. Med. 359 (2008) 2641–2650.
[8] J.F. Wu, W. Shen, N.Z. Liu, G.L. Zeng, M. Yang, G.Q. Zuo, X.N. Gan, H. Ren, K.F. Tang, Down-regulation of Dicer in hepatocellular carcinoma, Med. Oncol. 28 (2011) 804–809.
[9] L. Han, A. Zhang, X. Zhou, P. Xu, G.X. Wang, P.Y. Pu, C.S. Kang, Downregulation of Dicer enhances tumor cell proliferation and invasion, Int. J. Oncol. 37 (2010) 299–305.
[10] J.J. Ho, J.L. Metcalf, M.S. Yan, P.J. Turgeon, J.J. Wang, M. Chalsev, T.N. Petruzziello-Pellegrini, A.K. Tsui, J.Z. He, H. Dhamko, H.S. Man, G.B. Robb, B.T. Teh, M. Ohh, P.A. Marsden, Functional importance of Dicer protein in the adaptive cellular response to hypoxia, J. Biol. Chem. 287 (2012) 29003–29020.
[11] A. Pandey, A.V. Podtelejnikov, B. Blagoev, X.R. Bustelo, M. Mann, H.F. Lodish, Analysis of receptor signaling pathways by mass spectrometry: identification of vav-2 as a substrate of the epidermal and platelet-derived growth factor receptors, Proc. Natl. Acad. Sci. U. S. A. 97 (2000) 179–184.
[12] R. Chaerkady, A. Pandey, Quantitative proteomics for identification of cancer biomarkers, Proteomics Clin. Appl. 1 (2007) 1080–1089.
[13] D.M. Walther, M. Mann, Accurate quantification of more than 4000 mouse tissue proteins reveals minimal proteome changes during aging, Mol. Cell. Proteomics 10 (2011). M110 004523.
[14] I.M. Ferrando, R. Chaerkady, J. Zhong, H. Molina, H.K. Jacob, K. Herbst-Robinson, B.M. Dancy, V. Katju, R. Bose, J. Zhang, A. Pandey, P.A. Cole, Identification of targets of c-Src tyrosine kinase by chemical complementation and phosphoproteomics, Mol. Cell. Proteomics 11 (2012) 355–369.
[15] M.A. Barbhuiya, N.A. Sahasrabuddhe, S.M. Pinto, B. Muthusamy, T.D. Singh, V. Nanjappa, S. Keerthikumar, B. Delanghe, H.C. Harsha, R. Chaerkady, V. Jalaj, S. Gupta, B.R. Shrivastav, P.K. Tiwari, A. Pandey, Comprehensive proteomic analysis of human bile, Proteomics 11 (2011) 4443–4453.
[16] K. Kandasamy, A. Pandey, H. Molina, Evaluation of several MS/MS search algorithms for analysis of spectra derived from electron transfer dissociation experiments, Anal. Chem. 81 (2009) 7170–7180.
[17] T. Taus, T. Kocher, P. Pichler, C. Paschke, A. Schmidt, C. Henrich, K. Mechtler, Universal and confident phosphorylation site localization using phosphoRS, J. Proteome Res. 10 (2011) 5354–5362.
[18] W. Huang da, B.T. Sherman, R.A. Lempicki, Systematic and integrative analysis of large gene lists using DAVID bioinformatics resources, Nat. Protoc. 4 (2009) 44–57.
[19] R. Linding, L.J. Jensen, G.J. Ostheimer, M.A. van Vugt, C. Jorgensen, I.M. Miron, F. Diella, K. Colwill, L. Taylor, K. Elder, P. Metalnikov, V. Nguyen, A. Pasculescu, J. Jin, J.G. Park, L.D. Samson, J.R. Woodgett, R.B. Russell, P. Bork, M.B. Yaffe, T. Pawson, Systematic discovery of in vivo phosphorylation networks, Cell 129 (2007) 1415–1426.
[20] P. Longati, A. Bardelli, C. Ponzetto, L. Naldini, P.M. Comoglio, Tyrosines1234-1235 are critical for activation of the tyrosine kinase encoded by the MET proto-oncogene (HGF receptor), Oncogene 9 (1994) 49–57.
[21] S. Asada, T. Takahashi, K. Isodono, A. Adachi, H. Imoto, T. Ogata, T. Ueyama, H. Matsubara, H. Oh, Downregulation of Dicer expression by serum withdrawal sensitizes human endothelial cells to apoptosis, Am. J. Physiol. Heart Circ. Physiol. 295 (2008) H2512–H2521.
[22] S.L. Bellis, J.A. Perrotta, M.S. Curtis, C.E. Turner, Adhesion of fibroblasts to fibronectin stimulates both serine and tyrosine phosphorylation of paxillin, Biochem. J. 325 (Pt 2) (1997) 375–381.
[23] S. Sekine, R. Ogawa, R. Ito, N. Hiraoka, M.T. McManus, Y. Kanai, M. Hebrok, Disruption of Dicer1 induces dysregulated fetal gene expression and promotes hepatocarcinogenesis, Gastroenterology 136 (2009) 2304–2315 e2301–2304.
[24] L. Goyal, M.D. Muzumdar, A.X. Zhu, Targeting the HGF/c-MET pathway in hepatocellular carcinoma, Clin. Cancer Res. 19 (2013) 2310–2318.
[25] L. Yue, Y. Wang, H. Wang, H. Gao, J. Liang, A. Sui, J. Xiang, F. Zhou, C. Xu, W. Zhao, W. Liang, R. Yao, Inhibition of hepatocellular carcinoma cell growth by an anti-insulin-like growth factor-I receptor monoclonal antibody, Oncol. Rep. 28 (2012) 1453–1460.